



Cite this: *J. Anal. At. Spectrom.*, 2024, **39**, 592

Extending the application range of Hg isotopic analysis to sub- $\mu\text{g L}^{-1}$ levels using cold vapor generation multi-collector inductively coupled plasma-mass spectrometry with 10^{13} ohm Faraday cup amplifiers†

Laura Suárez-Criado,^a Eduardo Bolea-Fernandez,^b Lana Abou-Zeid,^b Mathias Vandermeiren,^b Pablo Rodríguez-González,^b Jose Ignacio Garcia Alonso^a and Frank Vanhaecke^a

High-precision determination of the isotopic composition of mercury (Hg) is of paramount importance for unraveling its biogeochemical cycle and for identifying the origin of Hg in environmental compartments. Cold vapor generation multi-collector inductively coupled plasma-mass spectrometry (CVG-MC-ICP-MS) is the standard approach for such application. Cold vapor generation provides a high Hg introduction efficiency into the ICP, while chromatographic Hg isolation is not required as a result of the selective reaction between Hg^{2+} and SnCl_2 . For environmental or biota samples with low Hg concentrations, however, this approach still presents challenges and reliable measurements typically require a Hg concentration $\geq 1 \mu\text{g L}^{-1}$ in the solution analyzed. Recent improvements of MC-ICP-MS instrumentation, including the introduction of the so-called Jet interface and $10^{13} \Omega$ Faraday cup amplifiers, enhance the signal-to-noise ratio. In this study, it was investigated to what extent this allows Hg isotopic analysis at lower concentration. Performance in Hg isotopic analysis was compared using two different sets of cones (standard vs. Jet), two plasma conditions (wet vs. dry) and two amplifier types ($10^{11} \Omega$ vs. $10^{13} \Omega$). Satisfactory accuracy and precision were achieved at a Hg concentration down to $0.1 \mu\text{g L}^{-1}$ in the solution measured when using Jet cones, dry plasma conditions, and the four available $10^{13} \Omega$ amplifiers. The uncertainty expressed as 2SD for the $\delta^{202}\text{Hg}$ values measured for the in-house standard solution was $\pm 0.2\%$ at $0.25 \mu\text{g Hg L}^{-1}$ and $\pm 0.3\%$ at $0.1 \mu\text{g Hg L}^{-1}$. The method was subsequently applied to the analysis of real surface water samples contaminated with toxic metals.

Received 23rd November 2023
 Accepted 11th January 2024

DOI: 10.1039/d3ja00414g

rsc.li/jaas

1. Introduction

Mercury (Hg) is a toxic metal that is globally distributed in the environment due to both natural processes and (especially) anthropogenic activities.¹ Elemental Hg can persist in the atmosphere for over half a year, can travel long distances and be deposited far from its original sources.² Mercury has seven stable isotopes – ^{196}Hg (0.15%), ^{198}Hg (9.97%), ^{199}Hg (16.87%), ^{200}Hg (23.10%), ^{201}Hg (13.18%), ^{202}Hg (29.86%) and ^{204}Hg (6.87%) – and during chemical, biological and physical

processes they may undergo natural isotope fractionation. This isotope fractionation gives rise to small variations in the natural isotopic composition of Hg. Mercury is one of the few elements for which both mass-dependent and mass-independent isotope fractionation (MDF and MIF, respectively) occur.³ Hg isotope ratio data are typically reported following the recommendation of Blum and Bergquist using the delta ($\delta^{\text{xxx}}\text{Hg}$ in ‰) and capital delta ($\Delta^{\text{xxx}}\text{Hg}$ in ‰) notations relative to NIST (National Institute for Standards and Technology, USA) SRM 3133 standard reference material.⁴ The combination of the $\delta^{\text{xxx}}\text{Hg}$ and $\Delta^{\text{xxx}}\text{Hg}$ values involving the different Hg isotopes provides valuable information for identifying sources of Hg pollution and for unravelling biogeochemical pathways of Hg in different environmental compartments.⁵

Traditionally, high-precision Hg isotopic analysis is carried out using multi-collector inductively coupled plasma-mass spectrometry (MC-ICP-MS) using cold vapor generation (CVG) for sample introduction.⁶ CVG provides a very high analyte introduction efficiency owing to the highly efficient

^aUniversity of Oviedo, Department of Physical and Analytical Chemistry, Julián Clavería 8, 33006-Oviedo, Spain

^bGhent University, Department of Chemistry, Atomic & Mass Spectrometry – A&MS Research Unit, Campus Sterre, Krijgslaan 281 – S12, 9000 Ghent, Belgium. E-mail: Frank.Vanhaecke@UGent.be

^cUniversity of Zaragoza, Aragón Institute of Engineering Research (I3A), Department of Analytical Chemistry, Zaragoza, Spain

† Electronic supplementary information (ESI) available. See DOI: <https://doi.org/10.1039/d3ja00414g>



reaction between Hg^{2+} and the reductant (typically SnCl_2 or NaBH_4), theoretically enabling an analyte introduction efficiency of (nearly) 100% into the ICP ion source.⁷ Moreover, chromatographic isolation of Hg prior to isotopic analysis using MC-ICP-MS is not necessary when using CVG with SnCl_2 as separation of Hg from the concomitant matrix is accomplished in the CVG device. In general, previous studies reporting Hg isotopic compositions were limited to samples with a Hg concentration $>1 \mu\text{g L}^{-1}$ due to insufficient precision at lower analyte concentration, although the measurement of the Hg isotopic composition of marine samples at a concentration level of $0.25 \mu\text{g L}^{-1}$ using $10^{12} \Omega$ Faraday cup amplifiers has been reported on.⁸

CVG-MC-ICP-MS enables accurate and precise Hg isotopic analysis at concentration levels down to $1 \mu\text{g L}^{-1}$ Hg, but the analysis of samples with an even lower Hg concentration level remains a challenging task. To overcome these issues, some studies have used preconcentration strategies using a chromatographic technique,^{9,10} a gold trap,¹¹ or activated carbon trap.¹² However, these preconcentration procedures make Hg isotopic analysis even more labor-intensive and enhance the risk of potential Hg isotope fractionation during the sample preparation protocol. Alternatively, also modification of the CVG unit has been reported to lead to higher sensitivity, thus enabling analysis of samples at a concentration level of $0.1 \mu\text{g L}^{-1}$ of Hg.¹³

Recent instrumental developments have enhanced the sensitivity of MC-ICP-MS instrumentation. First, the ion transmission efficiency was improved by enhancing the ion extraction efficiency, which is influenced by extraction and acceleration voltages, geometries of sampling and skimmer cones and interface pressure. For example, Thermo Fisher Scientific equipped their MC-ICP-MS instruments with a so-called 'Jet interface', that uses a high-performance pump to improve the interface vacuum, and geometrically modified sampling and skimmer cones (Jet sampler and X-type skimmer).¹⁴ Secondly, precision and accuracy of isotope ratios can be compromised by low-intensity ion beams, with the signal-to-noise ratio being affected by electronic baseline noise from the resistor in the amplifier feedback loop.¹⁵ Previously, for monitoring low-intensity ion beams, secondary electron multipliers (SEM) operated in ion counting mode were preferred over Faraday cup detectors, as SEMs are not affected by noise issues. However, SEMs suffer from variability in detection efficiency over time and beam intensity,¹⁵ while also requiring correction for detector dead time. This correction introduces an additional source of uncertainty.^{16,17} More recently however, $10^{13} \Omega$ Faraday cup amplifiers instead of standard $10^{11} \Omega$ ones were introduced, theoretically resulting in a 100-fold increase in output voltage and a 10-fold increase in the noise only, enhancing the signal-to-noise ratio by an order of magnitude, or an experimentally documented factor of 5–10.^{18,19}

To the best of our knowledge, the combination of a Jet interface and $10^{13} \Omega$ amplifiers has not been previously evaluated for measuring Hg isotope ratios in samples with low Hg concentrations ($<1 \mu\text{g L}^{-1}$). In this study, the accuracy and

precision attainable in Hg isotopic analysis using CVG-MC-ICP-MS were evaluated with different combinations of standard or Jet cones, with $10^{11} \Omega$ or $10^{13} \Omega$ amplifiers, and with wet (achieved through the continuous nebulization of an aqueous Tl isotopic standard for mass bias correction) and dry plasma conditions. An optimized protocol for analyzing the Hg isotopic composition in samples with low Hg content ($<1 \mu\text{g L}^{-1}$) is proposed. The methodology was validated by analyzing the secondary standard reference material UM-Almaden and applied to surface water samples from three locations contaminated with toxic metals.

2. Experimental

2.1 Reagents and materials

A pro-analysis purity level solution of $\text{SnCl}_2 \cdot 2\text{H}_2\text{O}$ (Sigma-Aldrich, UK, 3% SnCl_2 in 1.2 M HCl) was prepared for reducing Hg^{2+} to $\text{Hg}(0)$. High-purity Milli-Q H_2O ($>18.2 \text{ M}\Omega \text{ cm}$) was obtained from a Milli-Q Element water purification system (Millipore, France), while pro-analysis 12 M HCl and 14 M HNO_3 (ChemLab, Belgium) were further purified by sub-boiling distillation using Savillex (USA) DST acid purification systems.

Standard solutions of Hg (NIST SRM 3133) and Tl (NIST SRM 997) from the National Institute of Standards and Technology were used for external and internal correction for the mass bias caused by instrumental mass discrimination, respectively. A previously characterized in-house (IH) standard solution of Hg (Inorganic Ventures, The Netherlands, Lot: F2-HG02105) was used for optimization, method development and validation purposes.⁶ The UM-Almaden secondary reference material (NIST RM 8610) was also used for assessing the accuracy and precision in Hg isotope ratio measurements.

2.2 Instrumentation and measurements

An HGX-200 Cold Vapor and Hydride Generation system (Teledyne Cetac Technologies, USA) was used for Hg vapour generation and its introduction into the ICP of a Neptune XT MC-ICP-MS unit (Thermo Fisher Scientific, Germany), equipped with a high-transmission Jet interface. Two different sets of cones were evaluated: (i) a Jet-type Ni sampling cone and an X-type Ni skimmer cone, and (ii) a standard Ni sampling cone and an H-type Ni skimmer cone (Thermo Fisher Scientific, Germany). For simplicity, these two combinations will be referred to as (i) Jet cones and (ii) standard cones.

A combination of a $100 \mu\text{L min}^{-1}$ PFA concentric nebulizer and a spray chamber with cyclonic and Scott-type sub-units was used for continuous nebulization of a $5 \mu\text{g L}^{-1}$ Tl standard solution relied on for internal correction for instrumental mass discrimination. Fig. 1 provides a diagram of the instrumental set-up used in this work, illustrating the mixing of the sample flows obtained by CVG (Hg) and pneumatic nebulization (Tl) in a 'T piece'.

The operating conditions of the Neptune XT MC-ICP-MS unit are summarized in Table 1. The Faraday cups L3, L2, L1, C and



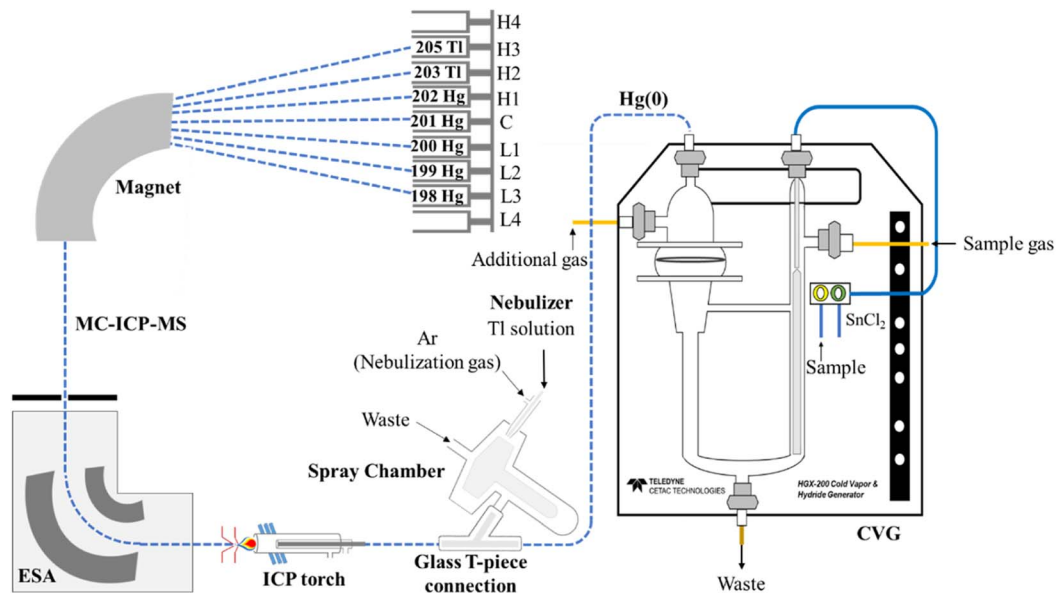


Fig. 1 Schematic representation of a CVG-MC-ICP-MS setup operated in wet plasma conditions.

H1 were used to monitor the signals of the Hg isotopes ^{198}Hg , ^{199}Hg , ^{200}Hg , ^{201}Hg and ^{202}Hg , respectively, while the Faraday cups H2 and H3 were used to monitor the signals for ^{203}Tl and ^{205}Tl (under wet plasma conditions only). Different amplifier configurations were evaluated as indicated in Table 1: (i) $10^{11}\ \Omega$ amplifiers for each Faraday cup, (ii) $10^{11}\ \Omega$ amplifiers for Faraday cups L2, L1, H1, H2 and H3 and $10^{13}\ \Omega$ ones for Faraday cups L3 and C, and (iii) $10^{11}\ \Omega$ amplifiers for Faraday cups L1, H2 and H3 and $10^{13}\ \Omega$ ones for Faraday cups L3, L2, C and H1. During the course of this work, two additional $10^{13}\ \Omega$ amplifiers (resulting in a total of 4) were installed, which explains why conditions (ii) and (iii) were evaluated. Prior to every measurement session, the software automatically performed a routine gain calibration and baseline integration during approximately 630 s. The use of Tau correction was also explored to address

amplifier decay disparities since this could be more relevant in the case of the $10^{13}\ \Omega$ amplifiers.²⁰ The correction was carried out automatically using the MC-ICP-MS software.

Total mercury (THg) concentrations were determined using an Agilent 8800 tandem ICP-mass spectrometer (ICP-MS/MS, Agilent Technologies, Japan). The sample introduction system consisted of a $400\ \mu\text{L}\ \text{min}^{-1}$ MicroMist nebulizer, mounted onto a Peltier-cooled ($2\ ^\circ\text{C}$) Scott-type spray chamber. The ICP-MS/MS instrument was operated in single-quadrupole (SQ) mode, whereby Q1 was used as an ion guide, and the collision/reaction cell (CRC) in “no gas” or “vented” mode. Quantification was accomplished *via* external calibration (calibration curve) with Tl as an internal standard to correct for potential matrix effects, instrument drift, and/or plasma instability.

Table 1 Instrument settings and data acquisition parameters for MC-ICP-MS Hg isotopic analysis

Neptune XT MC-ICP-MS				
Instrument settings	Wet plasma conditions		Dry plasma conditions	
RF power (W)	1250–1300		1250–1300	
Cool gas flow rate ($\text{L}\ \text{min}^{-1}$)	15		15	
Auxiliary gas flow rate ($\text{L}\ \text{min}^{-1}$)	1		1	
Nebulizer gas flow rate ($\text{L}\ \text{min}^{-1}$)	0.70–0.75		0.97–0.98	
Carrier gas flow rate ($\text{L}\ \text{min}^{-1}$)	0.25–0.30		0.14–0.15	
Additional gas flow rate ($\text{L}\ \text{min}^{-1}$)	0.03–0.04		—	
Sample uptake rate ($\text{mL}\ \text{min}^{-1}$)	0.7		0.7	
Tl standard solution uptake Tl rate ($\text{mL}\ \text{min}^{-1}$)	0.17		—	
SnCl_2 solution uptake rate ($\text{mL}\ \text{min}^{-1}$)	0.7		0.7	
Uptake time (s)	100		100	
Wash time (s)	150		150	
Mass resolution	Low resolution		Low resolution	
Mode	Static mode		Static mode	
Sampling cone	Standard	Jet cone	Standard	Jet cone
Skimmer cone	H-type	X-type	H-type	X-type



Data acquisition parameters						
Integration time (s)	4.194					
Blocks	5					
Cycles/block	10					
Total cycles	50					
Faraday cup configuration						
L3 (¹⁹⁸ Hg)	L2 (¹⁹⁹ Hg)	L1 (²⁰⁰ Hg)	C (²⁰¹ Hg)	H1 (²⁰² Hg)	H2 (²⁰³ Tl)	H3 (²⁰⁵ Tl)
(i) 10 ¹¹ Ω	10 ¹¹ Ω	10 ¹¹ Ω	10 ¹¹ Ω	10 ¹¹ Ω	10 ¹¹ Ω	10 ¹¹ Ω
(ii) 10 ¹³ Ω	10 ¹¹ Ω	10 ¹¹ Ω	10 ¹³ Ω	10 ¹¹ Ω	10 ¹¹ Ω	10 ¹¹ Ω
(iii) 10 ¹³ Ω	10 ¹³ Ω	10 ¹¹ Ω	10 ¹³ Ω	10 ¹³ Ω	10 ¹¹ Ω	10 ¹¹ Ω

2.3 Data treatment

When operating in wet plasma conditions, the bias caused by instrumental mass discrimination was corrected for using a combination of internal correction based on the Russell equation,²¹ using the continuously nebulized Tl standard solution (NIST SRM 997), and external correction relying on a NIST SRM 3133 Hg external standard measured in a sample-standard bracketing (SSB) approach. For dry plasma conditions, instrumental mass discrimination was corrected for by external correction only. For enabling adequate mass bias correction, the Hg concentration and acid content of all samples, standards and reference materials were matched (for the Hg concentration: within ±10%). After each measurement, a blank was run to avoid memory effects and ensure a sufficiently low background signal. The effect of blank subtraction was also evaluated.

MDF was reported in delta notation ($\delta^{XXX}\text{Hg}_{\text{‰}}$) relative to the NIST SRM 3133 standard⁴ using eqn (1):

$$\delta^{XXX}\text{Hg}_{\text{‰}} = \left(\frac{\left(\frac{XXX\text{Hg}}{^{198}\text{Hg}} \right)_{\text{sample}}}{\left(\frac{XXX\text{Hg}}{^{198}\text{Hg}} \right)_{\text{NIST SRM 3133}}} - 1 \right) \times 1000 \quad (1)$$

where XXX = 199, 200, 201 or 202.

MIF was reported in capital delta notation ($\Delta^{XXX}\text{Hg}_{\text{‰}}$) and was calculated from the corresponding measured $\delta^{XXX}\text{Hg}_{\text{‰}}$ values using eqn (2)–(4):⁴

$$\Delta^{201}\text{Hg} = \delta^{201}\text{Hg} - (\delta^{202}\text{Hg} \times 0.752) \quad (2)$$

$$\Delta^{200}\text{Hg} = \delta^{200}\text{Hg} - (\delta^{202}\text{Hg} \times 0.502) \quad (3)$$

$$\Delta^{199}\text{Hg} = \delta^{199}\text{Hg} - (\delta^{202}\text{Hg} \times 0.252) \quad (4)$$

2.4 Samples

In March 2023, surface water samples were collected from three different locations in Gijón (Asturias, Spain), using 50 mL Falcon tubes. For each water source, three separate water samples were taken, which were subsequently acidified with 2% (v/v) HCl. These samples were then stored at room temperature

prior to analysis. The water bodies under investigation – La Parra (A1), La Piquera (A2) and El Muselín (A3) – are all located in an industrialized area. The local water company in Gijón has declared these water sources unsafe for human consumption due to the presence of toxic metals. The total Hg concentration in the samples was determined using ICP-MS/MS by relying on external calibration using Tl as an internal standard. Mercury concentrations of approximately 3 $\mu\text{g L}^{-1}$ for A1, 1 $\mu\text{g L}^{-1}$ for A2 and 6 $\mu\text{g L}^{-1}$ for A3 were obtained.

3. Results and discussion

3.1 Evaluation of the instrumental set-up

3.1.1 Comparison of two different sampling and skimmer cone combinations. The accuracy and precision of results obtained using the two different sets of cones (standard cones and Jet cones) were evaluated at concentration levels ranging from 0.5 to 5.0 $\mu\text{g L}^{-1}$. The data acquisition parameters (integration time, number of blocks and of cycles/block) were selected based on previously optimized values.⁶ The $\delta^{XXX}\text{Hg}$ values for the IH standard were compared with those from a previous study reporting data obtained at 10 $\mu\text{g L}^{-1}$ Hg.¹⁸

Fig. 2 illustrates the average $\delta^{XXX}\text{Hg}_{\text{‰}}$ values ($n = 5$) for the IH standard obtained with both cone configurations at concentrations of 5.0, 2.5, 1.0 and 0.5 $\mu\text{g L}^{-1}$ Hg. The values presented in Fig. 2 were acquired under wet plasma conditions using 10¹¹ Ω amplifiers and are provided as an example. Similar observations were made with the different settings evaluated, as observed in Tables S1–S4† for $\delta^{202}\text{Hg}$, $\delta^{201}\text{Hg}$, $\delta^{200}\text{Hg}$ and $\delta^{199}\text{Hg}$, respectively. As can be observed in Fig. 2, the average values obtained using both configurations did not show significant differences at the different concentration levels evaluated. However, for the $\delta^{201}\text{Hg}$ value, better agreement with the IH standard reference value was achieved with the Jet cones configuration for two measurement sessions. In general, using Jet cones resulted in a better precision. Measurement results after blank subtraction can be found in Table S5.† Broadly speaking, there is minimal difference between values with and without blank subtraction, which indicates that the effect of the blank can be considered negligible within the experimental precision.

Table 2 shows the internal precision, expressed as average relative standard deviation (RSD, %) and SD for the Hg isotope ratios obtained from six measurements of a 1.0 $\mu\text{g L}^{-1}$ NIST SRM 3133 solution under various configurations. As can be seen, better internal precision was achieved for all Hg isotope ratios when measurements were conducted with the Jet cones (RSD% values ranging from 0.0048 to 0.0055% in comparison to the RSD% values obtained with the standard cones ranging from 0.0074 to 0.082%). The average RSD% values for the isotope ratios obtained from measurements at decreasing concentrations can be found in Table S6.† As the concentration level decreases, the average RSD% values increase.

3.1.2 Comparison of wet and dry plasma conditions. Experiments to compare the accuracy and precision of $\delta^{XXX}\text{Hg}$ values obtained under wet and dry plasma conditions were carried out. The results were acquired using the previously



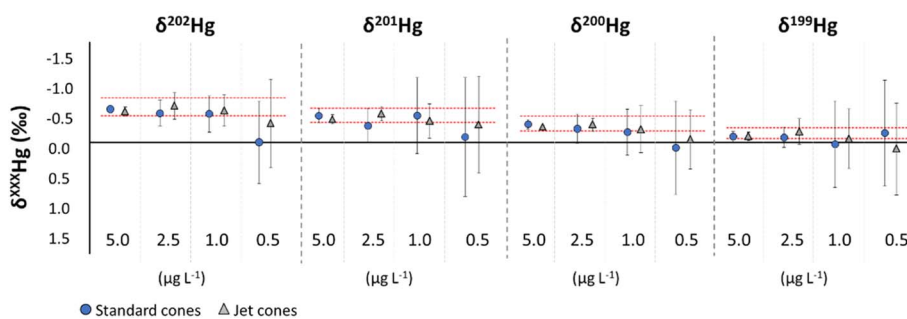


Fig. 2 Average $\delta^{\text{XXX}}\text{Hg}$ (‰) values for the IH standard ($n = 5$) obtained at different concentration levels with standard and jet cones under wet plasma conditions and using $10^{11} \Omega$ amplifiers. Red dashed lines represent the average $\pm 2\text{SD}$ for previously obtained IH values.⁶ Error bars correspond to 2SD and are obtained from $n = 5$ CVG-MC-ICP-MS measurements.

optimized data acquisition parameters⁶ across various concentration levels. The signal intensities in dry plasma conditions were approximately 2-fold higher than those observed in wet plasma conditions. For example, in dry plasma conditions, the ^{202}Hg signal intensities at a concentration level of $1 \mu\text{g L}^{-1}$ were $2.80 \times 10^{-13} \text{ A}$ (280 mV), while in wet plasma conditions, the signal intensity decreased to $1.77 \times 10^{-13} \text{ A}$ (177 mV).

The average $\delta^{\text{XXX}}\text{Hg}$ (‰) values ($n = 5$) for the IH standard obtained under both dry and wet plasma conditions at concentration levels ranging from 0.25 to $5.0 \mu\text{g L}^{-1}$ are shown in Fig. 3 and in Tables S1–S4.† Fig. 3 displays the values acquired with $10^{11} \Omega$ amplifiers and Jet cones under wet and dry plasma conditions. As expected, the 2SD values increase for both wet and dry plasma as the Hg concentration decreases. For most $\delta^{\text{XXX}}\text{Hg}$ (‰) values and concentration levels, a better agreement with the reference value is established in dry plasma conditions. According to the results shown in Table 2, the lowest RSD values were obtained in dry plasma conditions using the Jet cones configuration and $10^{11} \Omega$ amplifiers. Nonetheless, no significant differences in internal precision were found between the different configurations at a concentration of $1 \mu\text{g}$

L^{-1} Hg, even though signal intensities were higher in dry plasma conditions (Table 2). Table S6† also illustrates that the RSD values for the isotope ratio data increase as the concentration level decreases.

3.1.3 Comparison between $10^{11} \Omega$ and $10^{13} \Omega$ amplifiers.

Three different Faraday cup – amplifier configurations were tested. Initially, only two $10^{13} \Omega$ amplifiers were available, but by the end of this work, the MC-ICP-MS instrument was equipped with a total of four $10^{13} \Omega$ amplifiers. In the first configuration, all Faraday cups were connected to $10^{11} \Omega$ amplifiers. In the second configuration, the two $10^{13} \Omega$ amplifiers were connected to the Faraday cups monitoring the minor Hg isotopes ^{198}Hg and ^{201}Hg using Faraday cups L3 and C. In the third configuration, the signal intensities for all of the Hg isotopes of interest, except for ^{200}Hg , were collected in Faraday cups connected to $10^{13} \Omega$ amplifiers.

Fig. 4 provides a comparison of the average $\delta^{\text{XXX}}\text{Hg}$ (‰) values ($n = 5$) for the IH standard obtained with the three different amplifier setups under dry plasma conditions using the Jet cones configuration. It was observed that the $10^{13} \Omega$ amplifiers were saturated at concentration levels exceeding 1.0

Table 2 Average RSD (%) values and corresponding SDs for the Hg isotope ratios based on 6 measurements of a $1 \mu\text{g L}^{-1}$ NIST SRM 3133 standard solution as obtained using several configurations: two cone configurations (standard vs. Jet), two plasma conditions (wet vs. dry) and the three amplifier setups (i), (ii), and (iii) shown in Table 1

Cones	Plasma	Amplifiers		$^{199}\text{Hg}/^{198}\text{Hg}$	$^{200}\text{Hg}/^{198}\text{Hg}$	$^{201}\text{Hg}/^{198}\text{Hg}$	$^{202}\text{Hg}/^{198}\text{Hg}$	$^{205}\text{Tl}/^{203}\text{Tl}$
Standard	Wet	(i)	Average (%)	0.0077	0.0080	0.0082	0.0074	0.0019
			SD	0.0002	0.0005	0.0004	0.0005	0.0009
Standard	Wet	(ii)	Average (%)	0.0108	0.0100	0.0052	0.0094	0.0016
			SD	0.0020	0.0012	0.0006	0.0016	0.0001
Jet	Wet	(i)	Average (%)	0.0055	0.0050	0.0055	0.0048	0.0011
			SD	0.0004	0.0003	0.0006	0.0004	0.0001
Jet	Wet	(ii)	Average (%)	0.0075	0.0068	0.0041	0.0071	0.0014
			SD	0.0006	0.0007	0.0004	0.0007	0.0001
Jet	Dry	(i)	Average (%)	0.0043	0.0042	0.0046	0.0041	
			SD	0.0002	0.0005	0.0003	0.0005	
Jet	Dry	(ii)	Average (%)	0.0076	0.0076	0.0034	0.0078	
			SD	0.0017	0.0016	0.0002	0.0016	
Jet	Wet	(iii)	Average (%)	0.0040	0.0115	0.0044	0.0044	0.0030
			SD	0.0005	0.0015	0.0010	0.0003	0.0002
Jet	Dry	(iii)	Average (%)	0.0035	0.0132	0.0042	0.0045	
			SD	0.0003	0.0037	0.0008	0.0007	



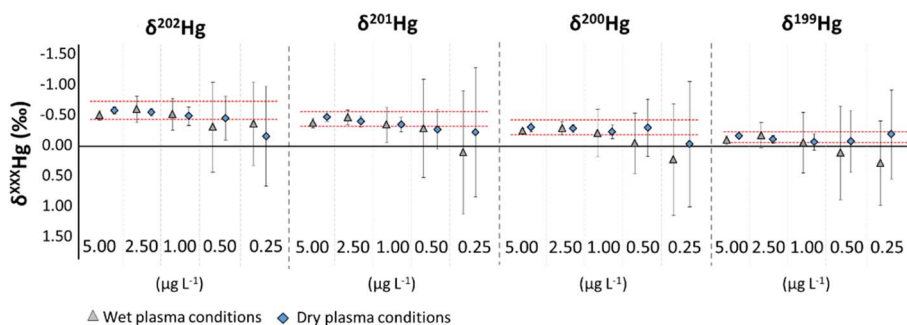


Fig. 3 Average $\delta^{\text{XXX}}\text{Hg}$ (‰) values for the IH solution ($n = 5$) obtained at different concentration levels under wet and dry plasma conditions using $10^{11}\ \Omega$ amplifiers and jet cones. Red dashed lines represent the average $\pm 2\text{SD}$ of the previously obtained IH values.⁶ Error bars correspond to 2SD and are obtained from $n = 5$ CVG-MC-ICP-MS measurements.

$\mu\text{g L}^{-1}$, and thus, the values obtained at concentration levels of 2.5 and $5.0\ \mu\text{g L}^{-1}$ Hg are shown for the first configuration only. It needs to be noted that the average $\delta^{200}\text{Hg}$ and $\delta^{201}\text{Hg}$ values for the IH standard obtained with the second and the third amplifier setup were otherwise collected under exactly the same instrumental conditions, and thus, the differences need to be attributed to variability between different measurement sessions. Notably, the accuracy and precision improved when more $10^{13}\ \Omega$ amplifiers were used, as seen in the $\delta^{199}\text{Hg}$ and $\delta^{202}\text{Hg}$ values. The average $\delta^{\text{XXX}}\text{Hg}$ (‰) values for the IH solution obtained under different instrument configurations are summarized in Tables S1–S4† for $\delta^{199}\text{Hg}$, $\delta^{200}\text{Hg}$, $\delta^{201}\text{Hg}$ and $\delta^{202}\text{Hg}$, respectively. With the third amplifier configuration (using four $10^{13}\ \Omega$ amplifiers) under dry plasma conditions and with Jet cones, the average isotope ratio results for the IH standard solution obtained at a concentration level of $0.5\ \mu\text{g L}^{-1}$ are similar to the values from another study obtained at a concentration of $10\ \mu\text{g L}^{-1}$.⁶ This represents a significant improvement, since it allows for the determination of the Hg isotopic composition of samples containing 20-fold lower Hg concentrations with the same level of precision.

The average RSD (%) of the isotope ratio measurements increased significantly when two different amplifiers were combined for the collection of the ^{198}Hg and $^{\text{XXX}}\text{Hg}$ isotopes, respectively, compared to the average RSD (%) values when only one type of amplifier was used (Table 2). Please note that, in

amplifier configuration (ii), $^{199}\text{Hg}/^{198}\text{Hg}$, $^{200}\text{Hg}/^{198}\text{Hg}$ and $^{202}\text{Hg}/^{198}\text{Hg}$ isotope ratios are calculated on the basis of data obtained combining two amplifier types, while in amplifier configuration (iii), only for the $^{200}\text{Hg}/^{198}\text{Hg}$ isotope ratio data obtained using two amplifier types were used.

The effect of tau correction was evaluated to address differences in the detector response time when a combination of both amplifier types was used. However, no significant differences were observed, nor for the $\delta^{\text{XXX}}\text{Hg}$ (‰) values neither for the RSD (%) of the Hg isotope ratios, as shown in Table S7.†

3.2 Evaluation of the data acquisition parameters

To assess the impact of data acquisition parameters on isotope ratio measurements with $10^{13}\ \Omega$ amplifiers, the integration time was decreased, while the number of cycles was increased. According to the literature,²² only the final number of cycles, rather than the number of blocks, affects the accuracy and precision of isotope ratio measurements. Consequently, two acquisition methods: the previously optimized method (4.194 s integration time, 5 blocks and 1 cycle)⁶ and a second method (2.097 s integration time, 1 block and 100 cycles) were evaluated and the corresponding data compared. The accuracy and internal precision of the results were assessed by measuring an IH standard solution at a concentration level of $1\ \mu\text{g L}^{-1}$ Hg. Table 3 shows that better accuracy and internal precision were

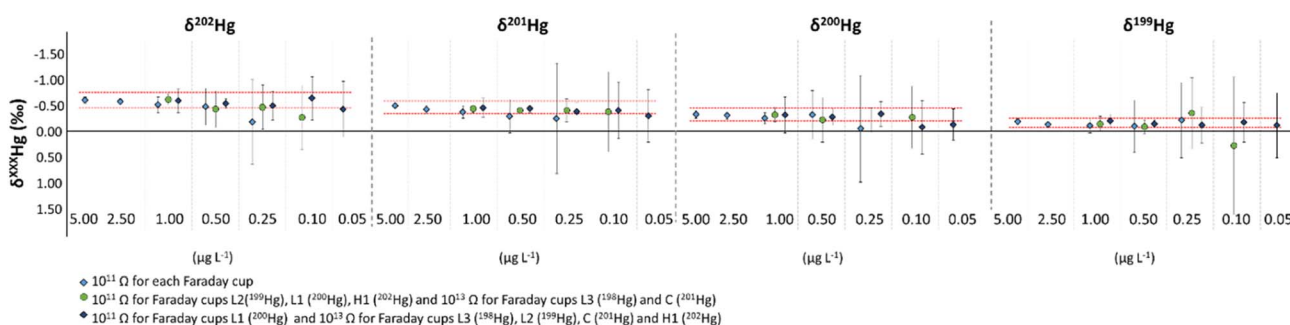


Fig. 4 Average $\delta^{\text{XXX}}\text{Hg}$ (‰) values for the IH solution ($n = 5$) obtained at different concentration levels under dry plasma conditions, with Jet cones and using the three different amplifier configurations (i), (ii), and (iii) described in Table 1. Red dashed lines represent the average $\pm 2\text{SD}$ of the previously obtained IH values.⁶ Error bars correspond to 2SD and are obtained from $n = 5$ CVG-MC-ICPMS measurements.



achieved with the first method, which was already applied to compare the effect of different instrumental settings.

3.3 Evaluation of the required extent of matching of analyte concentrations of sample and standard solution

For the proper application of the external correction for the mass bias, it is essential to ensure that the signal intensities for sample and external standard solution do not have a mismatch >10%.²³ To determine the extent to which mismatching affects the accuracy of Hg isotope ratio measurements at low concentration levels, experiments were carried out with varying levels of analyte concentration mismatching between the IH standard and the NIST SRM 3133 solutions at a concentration level of 0.25 $\mu\text{g L}^{-1}$ Hg, analyzed using the optimal configuration and data acquisition parameters. Fig. 5 illustrates that the worst accuracy is observed at a $\pm 20\%$ mismatch. The discrepancies observed when the Hg concentration in the external standard is matched within $\pm 10\%$ of that of the sample (*i.e.*, IH standard solution) can be attributed to the instrument's inherent variability.

3.4 Evaluation of external precision

One of the main goals of this work was to develop a methodology for determining the isotopic composition of Hg in samples with low Hg concentration. After selecting the optimal instrumental configuration (*i.e.*, use of four 10^{13} Ω amplifiers, Jet cones, and dry plasma conditions) and data acquisition parameters, the concentration level at which reliable results can still be obtained was evaluated.

The accuracy and precision of the $\delta^{\text{xxx}}\text{Hg}$ (‰) values ($n = 20$) for the IH standard at concentration levels ranging from 1.0 to 0.1 $\mu\text{g L}^{-1}$ were evaluated. Table 4 shows that the highest 2SD values were obtained for $\delta^{200}\text{Hg}$, especially at lower concentration levels (*i.e.*, 0.25 and 0.10 $\mu\text{g L}^{-1}$). This can be attributed to the monitoring of the ^{200}Hg ion beam using a Faraday cup connected to a 10^{11} Ω amplifier. Self-evidently, the 2SD values increase as the Hg concentration levels decrease. However, at the 0.25 $\mu\text{g L}^{-1}$ concentration level, the $\delta^{\text{xxx}}\text{Hg}$ values remain similar to those obtained at 0.50 and 1.0 $\mu\text{g L}^{-1}$ Hg, as well as those reported in an earlier study⁶ carried out at 10 $\mu\text{g L}^{-1}$ Hg concentration level and ranging from 0.13 to 0.27‰. At the 0.10 $\mu\text{g L}^{-1}$ concentration level, the 2SD values are below 0.50, which is consistent with results obtained from relatively short

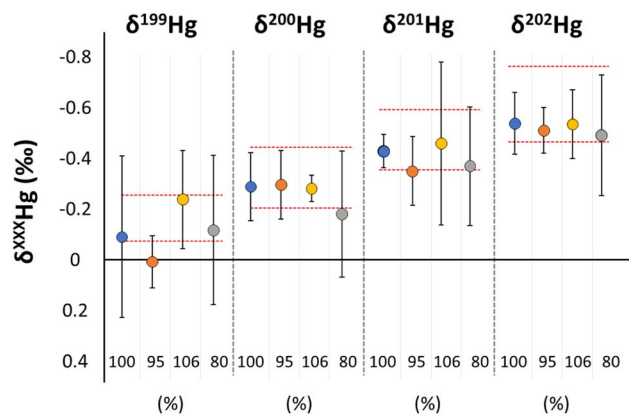


Fig. 5 Average $\delta^{\text{xxx}}\text{Hg}$ (‰) values for the IH standard ($n = 5$) obtained at different extents of Hg concentration mismatch between the IH standard solution and the NIST SRM 3133 standard solution at a concentration level of 0.25 $\mu\text{g L}^{-1}$ Hg. The red dashed lines represent the average $\pm 2\text{SD}$ of the previously obtained IH values.⁶ Error bars correspond to 2SD and are obtained from $n = 5$ CVG-MC-ICPMS measurements. Blue circles represent 100% matching, orange circles represent 95% matching, yellow circles represent 106% matching, and grey circles 80% matching.

transient signals during species-specific Hg isotopic analysis *via* gas chromatography (GC) MC-ICP-MS analysis.²⁴ Considering the SD, the average $\delta^{\text{xxx}}\text{Hg}$ results were found to be in good agreement with the reference values⁶ at Hg concentration levels as low as 0.1 $\mu\text{g L}^{-1}$.

Additionally, a long-term stability study (7 months) was carried out using the IH mercury standard measured at 0.25 $\mu\text{g L}^{-1}$ ($n = 51$). The values found are also included in Table 4 and agree with the literature values.⁶

3.5 Hg isotopic analysis of samples with low Hg concentration

The NIST RM 8610 secondary reference standard was analysed at a concentration level of 0.25 $\mu\text{g L}^{-1}$ Hg using the optimal instrumental configuration and data acquisition parameters, *i.e.* with Jet cones, dry plasma conditions, and all four available 10^{13} Ω amplifiers. The resulting average $\delta^{\text{xxx}}\text{Hg}$ (‰) and $\Delta^{\text{xxx}}\text{Hg}$ (‰) values from $n = 10$ measurements can be found in Table 5. As can be seen, the values for both $\delta^{\text{xxx}}\text{Hg}$ (‰) and

Table 3 Comparison of the average $\delta^{\text{xxx}}\text{Hg}$ (‰) values for the IH standard ($n = 5$) and average SD and RSD (%) values for the Hg isotope ratio results for NIST SRM 3133 ($n = 6$) and SD obtained at a concentration level of 1 $\mu\text{g L}^{-1}$ Hg with two different data acquisition parameter sets: method 1 (4.194 s integration time, 5 blocks and 1 cycle) and Method 2 (2.097 s integration time, 1 block and 100 cycles)

Method		$\delta^{199}\text{Hg}$	$\delta^{200}\text{Hg}$	$\delta^{201}\text{Hg}$	$\delta^{202}\text{Hg}$	$^{199}\text{Hg}/^{198}\text{Hg}$	$^{200}\text{Hg}/^{198}\text{Hg}$	$^{201}\text{Hg}/^{198}\text{Hg}$	$^{202}\text{Hg}/^{198}\text{Hg}$
						RSD (%)	RSD (%)	RSD (%)	RSD (%)
IH (literature values) ⁶	Average	-0.14	-0.30	-0.45	-0.59	—	—	—	—
	SD	0.05	0.06	0.06	0.08	—	—	—	—
Method 1	Average	-0.13	-0.34	-0.44	-0.56	0.0028	0.0126	0.0039	0.0037
	SD	0.03	0.05	0.04	0.03	0.0005	0.0012	0.0005	0.0003
Method 2	Average	-0.10	-0.20	-0.36	-0.51	0.0029	0.0202	0.0047	0.0046
	SD	0.05	0.07	0.05	0.06	0.0001	0.0015	0.0005	0.0004



Table 4 Average $\delta^{xxx}\text{Hg}$ (‰) ($n = 20$ or $n = 51$ as indicated) values and 2SD for the IH standard at different Hg concentration levels

	$\delta^{199}\text{Hg} \pm 2\text{SD}$	$\delta^{200}\text{Hg} \pm 2\text{SD}$	$\delta^{201}\text{Hg} \pm 2\text{SD}$	$\delta^{202}\text{Hg} \pm 2\text{SD}$
IH (literature values) ⁶	-0.14 ± 0.09	-0.30 ± 0.12	-0.45 ± 0.12	-0.59 ± 0.15
$1 \mu\text{g L}^{-1}$	-0.12 ± 0.10	-0.25 ± 0.10	-0.41 ± 0.10	-0.54 ± 0.09
$0.5 \mu\text{g L}^{-1}$	-0.10 ± 0.12	-0.22 ± 0.16	-0.37 ± 0.13	-0.47 ± 0.14
$0.25 \mu\text{g L}^{-1}$	-0.11 ± 0.14	-0.20 ± 0.27	-0.39 ± 0.13	-0.50 ± 0.18
$0.1 \mu\text{g L}^{-1}$	-0.09 ± 0.31	-0.17 ± 0.49	-0.34 ± 0.31	-0.54 ± 0.34
$0.25 \mu\text{g L}^{-1}$ ($n = 51$)	-0.13 ± 0.15	-0.25 ± 0.21	-0.40 ± 0.20	-0.54 ± 0.20

Table 5 Hg isotope ratios in the secondary standard NIST RM 8610 (Hg concentration of $0.25 \mu\text{g L}^{-1}$)

	$\delta^{199}\text{Hg}$	$\delta^{200}\text{Hg}$	$\delta^{201}\text{Hg}$	$\delta^{202}\text{Hg}$	$\Delta^{199}\text{Hg}$	$\Delta^{201}\text{Hg}$
Mead <i>et al.</i> ²⁵	-0.15	-0.29	-0.44	-0.58	-0.01	-0.02
2SD	0.06	0.06	0.08	0.08	0.05	0.03
Blum <i>et al.</i> ⁴	-0.14	-0.27	-0.44	-0.54	-0.01	0.04
2SD	0.06	0.04	0.07	0.08	0.02	0.04
This study	-0.16	-0.33	-0.51	-0.66	0.00	-0.02
2SD	0.21	0.12	0.14	0.13	0.19	0.10

$\Delta^{xxx}\text{Hg}$ (‰) are in line with the values obtained by Mead *et al.*²⁵ and Blum *et al.*,⁴ which validates the proposed methodology.

Additionally, three surface water samples diluted to achieve solutions with a Hg concentration of $0.25 \mu\text{g L}^{-1}$ were analyzed as a proof-of-concept application. The resulting $\delta^{xxx}\text{Hg}$ (‰) and $\Delta^{xxx}\text{Hg}$ (‰) values obtained for each sample are presented in Table 6. In general, higher 2SD values were obtained for $\delta^{200}\text{Hg}$, consistent with the trend observed throughout this study. Despite the geographical proximity of the sources, significant differences were found; especially the δ -values for the first water source (A1) were significantly lower than those for the other two samples. The $\delta^{202}\text{Hg}$ (‰) and $\Delta^{199}\text{Hg}$ (‰) values obtained for the three water sources are in agreement with values for freshwaters containing Hg of mixed sources as reported in a review by Blum, Sherman and Johnson.³ Based on the delta values of the three water sources, we could hypothesize that the Hg

contamination in water samples from A2 (La Piquera) and A3 (El Muselín) comes from the same source, while in the case of the water samples from A1 (La Parra), the source would be different. Accurate knowledge of the source of Hg polluting the water sources could solve the problem by making them safe for human consumption again.

4. Conclusions

In this work, a systematic comparison of the capabilities and limitations of various instrumental configurations and data acquisition parameters for the determination of Hg isotope ratios at Hg concentration levels down to $0.1 \mu\text{g L}^{-1}$ was carried out. The assessment encompassed the evaluation of two cone setups (standard and Jet), two plasma conditions (wet and dry), and two Faraday cup amplifier types ($10^{11} \Omega$ and $10^{13} \Omega$). The combination of two different amplifiers for the collection of the ^{xxx}Hg and ^{198}Hg isotopes resulted in the least favorable internal precisions. The impact of tau correction was found to be negligible. At the lowest concentration levels, the most favorable results were achieved through the use of Jet cones, dry plasma conditions, and all four available $10^{13} \Omega$ amplifiers available in the set-up used. This configuration yielded accuracy and precision at the $0.25 \mu\text{g L}^{-1}$ Hg concentration level similar to values reported in a previous study at the much higher concentration level of $10 \mu\text{g L}^{-1}$ Hg.⁶ At the $0.1 \mu\text{g L}^{-1}$ concentration level, the standard deviations were still within the acceptable range for Hg isotope ratio measurements resulting from transient signals.²⁴ As a proof-of-concept, the method developed was used for the determination of the isotopic composition of Hg in the secondary reference standard NIST RM 8610 and in real water samples, diluted to a concentration level of $0.25 \mu\text{g L}^{-1}$ Hg. The mean delta values obtained for NIST RM 8610 were consistent with the values obtained in other studies.^{4,25} The 2SD values obtained for the real water samples were comparable to those achieved at higher concentrations, highlighting the method's robustness and applicability to samples characterized by low Hg concentration.

Conflicts of interest

There are no conflicts to declare.

Acknowledgements

Laura Suárez-Criado acknowledges the Principality of Asturias, Spain, for their financial support through the Severo Ochoa

Table 6 Hg isotope ratio results for real surface water samples (Hg concentrations of approximately $0.25 \mu\text{g L}^{-1}$)

Water source	$\delta^{199}\text{Hg}$	$\delta^{200}\text{Hg}$	$\delta^{201}\text{Hg}$	$\delta^{202}\text{Hg}$	$\Delta^{199}\text{Hg}$	$\Delta^{201}\text{Hg}$
A 1.1.	-0.53	-0.81	-1.30	-1.43	-0.16	-0.22
A 1.2.	-0.52	-0.74	-1.24	-1.42	-0.16	-0.18
A 1.3.	-0.46	-0.63	-1.35	-1.39	-0.11	-0.30
Average	-0.50	-0.72	-1.30	-1.42	-0.14	-0.23
2SD	0.07	0.18	0.11	0.04	0.06	0.13
A 2.1.	-0.20	-0.16	-0.42	-0.51	-0.07	-0.04
A 2.2.	-0.20	-0.13	-0.47	-0.53	-0.06	-0.07
A 2.3.	-0.23	-0.25	-0.49	-0.58	-0.08	-0.05
Average	-0.21	-0.18	-0.46	-0.54	-0.07	-0.05
2SD	0.03	0.12	0.07	0.07	0.02	0.04
A 3.1.	-0.33	-0.01	-0.52	-0.66	-0.16	-0.03
A 3.2.	-0.33	-0.16	-0.44	-0.60	-0.18	0.01
A 3.3.	-0.32	-0.23	-0.68	-0.66	-0.15	-0.19
Average	-0.33	-0.14	-0.55	-0.64	-0.16	-0.07
2SD	0.02	0.22	0.24	0.06	0.03	0.21



scholarship ref. BP19-131 and the Banco Santander for the financial support through “Ayudas de movilidad de excelencia para docentes e investigadores”. The Spanish Ministry of Science and Innovation is acknowledged for the funding through Project MCIU-22-PID2021-125795NB-I00. The authors would also like to thank José Ignacio Calvelo Chouza (Empresa Municipal de Aguas de Gijón S. A.) for the assistance provided during sample collection. E. B.-F. acknowledges financial support from the Ramón y Cajal programme (RYC2021-031093-I) funded by MCIN/AEI/10.13039/501100011033 and the European Union (NextGenerationEU/PRTR), the grant PID2021-122455NB-I00, funded by MCIN/AEI/10.13039/501100011033 and by “ERDF A way of making Europe”, and also the Aragón Government (DGA, Construyendo Europa desde Aragón, Grupo E43_20R). The Research Foundation FWO-Vlaanderen is acknowledged for providing the funding for the acquisition of the MC-ICP-MS instrumentation and its installation at the A&MS research group at Ghent University (ZW15-02 – G0H6216N).

References

- 1 W. F. Fitzgerald and T. W. Clarkson, *Environ. Health Perspect.*, 1991, **96**, 159–166.
- 2 N. E. Selin, *Annu. Rev. Environ. Resour.*, 2009, **34**, 43–63.
- 3 J. D. Blum, L. S. Sherman and M. W. Johnson, *Annu. Rev. Earth Planet. Sci.*, 2014, **42**, 249–269.
- 4 J. D. Blum and B. A. Bergquist, *Anal. Bioanal. Chem.*, 2007, **388**, 353–359.
- 5 H. Hintelmann, *Use of Stable Isotopes in Mercury Research, Mercury in the Environment: Pattern and Process*, ed. M. S. Bank, University of California Press, Berkeley, CA, 2012.
- 6 A. Rua-Ibarz, E. Bolea-Fernandez and F. Vanhaecke, *Anal. Bioanal. Chem.*, 2016, **408**, 417–429.
- 7 M. Shi, B. A. Bergquist, A. Zhou, Y. Zhao, R. Sun, J. Chen and W. Zheng, *J. Anal. At. Spectrom.*, 2023, **38**, 1076–1087.
- 8 M. Jiskra, L. E. Heimbürger-Boavida, M. M. Desgranges, M. V. Petrova, A. Dufour, B. Ferreira-Araujo, J. Masbou, J. Chmeleff, M. Thyssen, D. Point and J. E. Sonke, *Nature*, 2021, **597**(7878), 678–682.
- 9 J. Chen, H. Hintelmann and B. Dimock, *J. Anal. At. Spectrom.*, 2010, **25**, 1402–1409.
- 10 S. Bouchet, S. Bérail and D. Amouroux, *Anal. Chem.*, 2018, **90**, 7809–7816.
- 11 L. Yang, B. Yu, H. Liu, X. Ji, C. Xiao, Y. Liang, L. Hu, Y. Yin, J. Shi and G. Jiang, *J. Anal. At. Spectrom.*, 2022, **42**, 2480–2489.
- 12 K. Li, C. J. Lin, W. Yuan, G. Sun, X. Fu and X. Feng, *J. Anal. At. Spectrom.*, 2019, **34**, 2303–2313.
- 13 H. Geng, R. Yin and X. Li, *J. Anal. At. Spectrom.*, 2018, **33**, 1932–1940.
- 14 T. Breton, N. S. Lloyd, A. Trinquier, C. Bouman and J. B. Schwieters, *Procedia Earth Planet. Sci.*, 2015, **13**, 240–243.
- 15 J. M. Koornneef, C. Bouman, J. B. Schwieters and G. R. Davies, *Anal. Chim. Acta*, 2014, **819**, 49–55.
- 16 S. M. Nelms, C. R. Quétel, T. Prohaska, J. Vogl and P. D. Taylor, *J. Anal. At. Spectrom.*, 2001, **16**(4), 333–338.
- 17 F. Vanhaecke, G. De Wannemacker, L. Moens, R. Dams, C. Latkoczy, T. Prohaska and G. Stingeder, *J. Anal. At. Spectrom.*, 1998, **13**(6), 567–571.
- 18 J. M. Koornneef, I. Nikogosian, M. J. van Bergen, R. Smeets, C. Bouman and G. R. Davies, *Chem. Geol.*, 2015, **397**, 14–23.
- 19 R. Grigoryan, M. Costas-Rodríguez, P. Santens and F. Vanhaecke, *Anal. Chem.*, 2020, **92**, 15975–15981.
- 20 K. Yamamoto, H. Asanuma, H. Takahashi and T. Hirata, *J. Anal. At. Spectrom.*, 2021, **36**(3), 668–675.
- 21 L. Yang, *Mass Spectrom. Rev.*, 2009, **28**(6), 990–1011.
- 22 H. Hintelmann and S. Y. Lu, *Analyst*, 2003, **128**, 635–639.
- 23 R. Yin, D. P. Krabbenhoft, B. A. Bergquist, W. Zheng, R. F. Lepak and J. P. Hurley, *J. Anal. At. Spectrom.*, 2016, **31**, 2060–2068.
- 24 S. Queipo-Abad, P. Rodríguez-González and J. I. García Alonso, *J. Anal. At. Spectrom.*, 2019, **34**, 753–763.
- 25 C. Mead and T. M. Johnson, *Anal. Bioanal. Chem.*, 2010, **397**, 1529–1538.

